DISCRETE ELEMENT MODELING OF BLADE–STRIKE FREQUENCY AND SURVIVAL OF FISH PASSING THROUGH HYDROKINETIC TURBINES

Pedro Romero-Gomez
Pacific Northwest National Laboratory
Richland, WA. USA

Marshall C. Richmond[*]
Pacific Northwest National Laboratory
Richland, WA. USA

ABSTRACT

Evaluating the consequences to fish from blade-strike on marine hydrokinetic (MHK) turbine blades is important for incorporating environmental objectives into the integral optimization of machine performance. For instance, experience with conventional hydroelectric turbines has shown that innovative shaping of the blade and other machine components can improve hydraulic performance while reducing negative impacts to fish and other aquatic life. In this work, we used unsteady computational fluid dynamics (CFD) simulations of turbine flow and discrete element modeling (DEM) of particle motion to estimate the frequency and severity of collisions between a horizontal axis MHK tidal energy device and drifting aquatic organisms or debris. Two metrics are determined with the method: the strike frequency and the survival rate estimate. To illustrate the procedure step-by-step, an example case of a simple runner model was run and compared against a probabilistic model widely used for strike frequency evaluation. The results for the example case showed a strong correlation between the two approaches. In the application case of the actual MHK turbine flow, turbulent flow was modeled using detached eddy simulation (DES) in conjunction with a full moving rotor. The CFD-simulated power and thrust were satisfactorily comparable to experimental results conducted in a water tunnel on a reduced-scale (1:8.7) version of the turbine design. A cloud of DEM particles was injected into the domain to simulate fish or debris entrained into the turbine flow. Because various studies have pointed out the importance of fish volitional behavior, an assumed avoidance rate of 90% was applied to the particle sample. The strike frequency was the ratio of the count of colliding particles to the crossing sample size. The fish length and approaching velocity were test conditions in the simulations of the MHK turbine. Comparisons

showed that DEM-based frequencies tend to be greater than previous results from Lagrangian particles and probabilistic models, mostly because the DEM scheme accounts for both the geometric aspects of the passage event —which only the probabilistic method does— as well as the fluid-particle interactions —which only the Lagrangian particle method does. With the full particle sample (0% avoidance), the DEM-based survival rates were generally high (above 90% in all studied cases), and comparable to previously reported laboratory results for small fish but not for mid-size fish mainly because of the considerable differences in rotor design between the CFD and laboratory models. With an assumed avoidance rate of 90%, the survival rates increased to nearly 99% across all scenarios. These results point to the need for further research and development of field monitoring methods for operating turbines to better understand the potential interaction between fish and MHK devices. The modeling framework can be used for applications that aim at evaluating the biological performance of MHK turbine units during the design phase and to provide information to regulatory agencies needed for the environmental permitting process.

INTRODUCTION

Hydrokinetic power production is an emerging renewable technology of increasing interest to the research community and governmental entities for clean energy generation. The fundamental principle of hydrokinetic technology is to extract the energy from flowing currents by operating turbines at zero- or near zero-head hydraulic conditions [1–4]. Hydrokinetic turbines can therefore be installed and operated in tidal current sites, rivers, and estuaries. In the U.S.A. and Europe (the United Kingdom in particular), a large number of hydrokinetic projects have been initiated and developed to different stages: planning, site development, device testing, or deployment [5]. In the U.S.A.,

---

[*]Corresponding Author: marshall.richmond@pnnl.gov

the Federal Energy Regulatory Commission (FERC) is in charge of licensing new hydrokinetic projects, and regularly issues the most up-to-date information on the newly approved sites. As of January 2014, the FERC has issued 16 preliminary permits with an expected capacity of 216.7 MW [6]. This context shows the current and future importance of hydrokinetic technology, and the immediate need to develop processes to assess its impact on the environment. The present work evaluates the likelihood of fish striking a hydrokinetic device in marine environments, and the potential consequence in terms of fish survival.

In practice, the design of new hydrokinetic turbines is usually based on concepts of two consolidated fields [1, 2]: wind energy and propulsion systems. Whereas knowledge of hydrodynamic aspects is relatively abundant [2], studies specialized in the potential environmental impacts of hydrokinetic technology are more scarce. The biological performance —the interaction between hydrokinetic devices and living organisms— is particularly necessary because fish and other aquatic biota will potentially come into contact with hydrokinetic turbines as is the case, for instance, with birds and wind turbines. For that reason, a recent study compared hydrokinetic systems to conventional hydropower, and concluded that hydrokinetic systems may have superior biological performance because of the less abrupt change in flow direction and low approach velocities [7]. Another study conducted quantitative evaluations of survival rates of live fish during hydrokinetic turbine passage in a laboratory setting [8], and found relatively low mortality rates in various test conditions. Other studies have focused on the description of potential consequences of a tidal power project on fish passage [9], and fish injury and mortality from a device deployed in the field [10].

Although laboratory and field studies offer the advantage for directly evaluating the impacts of hydrokinetic technology on living fish, they can only be conducted after the design, construction and installation of devices. In addition, the compounding factors causing injury or mortality of fish during passage make it difficult to examine individual injury mechanisms, thereby preventing technology developers from taking measures for enhancing specific performance indicators. In this work, we present an alternative modeling approach consisting of two major steps: first, we characterize the detailed hydraulic conditions for hydrokinetic turbine flows, and second we evaluate the biological impacts of such conditions by selecting strike frequency and intensity as the examined stressor. We present our procedure with an illustrative case, and thereafter apply the method to a full-scale marine hydrokinetic (MHK) turbine unit at real-world operating conditions.

For the flow description, we conducted computational fluid dynamics (CFD) simulations of the MHK turbine flows under various operating conditions. Previous CFD studies have demonstrated the ability to accurately reproduce the flow environment surrounding operational hydrokinetic turbines. Some works have represented the turbine as a sink/source term in the momen-

tum and turbulence conservation equations [11–13], while others have described the full geometry features to provide a high resolution of transient hydraulic conditions [4, 14]. The former approach is less computational demanding and allows for flow descriptions over large domains useful for siting and optimization of an array of turbines. The latter, although more computationally expensive, is required to develop predictive evaluations of blade-strike frequency. The present work employed this latter flow-resolving approach to compute potential fish trajectories and interactions with moving blades. Composite particles were used to represent fish trajectories during turbine crossing. The particle displacements and rotations were solved with the discrete element modeling (DEM) approach that has widely been used in particulate flow simulations in geo-mechanics, powder technology, erosion, and sediment deposition [15]. The procedure in this study was carried over from previous studies conducted with spherical Lagrangian particles [16, 17].

The present study also included an evaluation of strike-related mortality, as well as the effect of the rate of avoidance as fish approach the hydrokinetic device. Previous studies have discussed the avoidance behavior and blade-strike mortality, and examined these issues in laboratory and field settings. One report from the Oak Ridge National Laboratory recognized that blade-strike probabilities are lower in hydrokinetic devices than in conventional hydropower, but argued that fish at early-life stages are at risk because of their lower ability to react and avoid operating turbines [5]. By using a probabilistic model revisited in the present study, they estimated blade-strike probabilities at different assumed avoidance rates, 10% and 50%. Another associated report summarized a number of existing and planned projects to identify potential of avoidance and attraction [18]. They suggested that species that prefer backwater habitats are less at blade-strike risk than those swimming in the main channel of rivers because hydrokinetic devices are normally situated in high-velocity regions. Although the study extensively identified most potential fish-structure interactions, it pointed to the need for laboratory and field studies to conclude on whether avoidance or attraction will prevail. Because passive individuals were identified to be at the highest risk, laboratory experiments on larval and juvenile fish (lengths ranging from 4-35 mm) crossing blade profiles were conducted to determine survival rates [19]. The design conditions were blade shape, entrainment velocity, fish species and age group. Among many findings, they calculated survival rates as low as 32.2% for 1-day-post-hatching striped bass at current velocity of 0.85 m/s, and 71.2% for age group 11-14 day-post-hatching, showing the influence of the developmental stage of fish on survival at the moment of crossing. A series of laboratory sponsored by the Electric Power Reseach Institute (EPRI) conducted experiments of fish behavior and survival rates across operating hydrokinetic turbines [8, 20], and derived a relationship of survival rate as a function of blade features and entrainment flow [21], which is used in this work. Lastly, a

field study using camera systems on a rocky reef at 9 m depth to record the behavior of fish passing through a region occupied by a vertical-axis hydrokinetic rotor [22]. The distributions of fish counts at different distances from the rotor center with and without the device showed that virtually no fish passed through the device in operation. To incorporate the avoidance rate into the present calculations, we assumed that 90% of modeled particles entirely avoided the runner, and computed the resulting blade-strike frequency and strike-related survival rate.

The organization of this article is as follows. First, two methods for strike frequency evaluation are presented: the kinematic probabilistic model and the DEM scheme. The equations of linear and angular motion of the DEM particles are outlined. Second, the method for estimating survival rates is briefly explained. Third, the example case is presented, where the fish model and a simple rotor model are introduced. The correlation between the kinematic probabilistic and DEM schemes is discussed. Next, the marine hydrokinetic turbine unit is described, as well as the CFD and particle simulation setups. The discussion includes the results from previous studies of the same turbine design at the same flow conditions, but with Lagrangian particles. Finally, conclusions and future research opportunities are provided at the end of the document.

STRIKE FREQUENCY ESTIMATE
Kinematic Probabilistic Modeling

The likelihood of fish striking rotating blades of hydropower turbines has been evaluated with a probabilistic model introduced more than fifty years ago [23]. In the most simplified form, two factors contribute to the total probability of strike (P): the strike probability owing to the leading edge (P_{stk}), and owing to the blade thickness (P_{blade}). P_{stk} results from dividing the fish travel time to pass the runner plane by the duration of gaps created between adjacent blades. Likewise, P_{blade} represents the exposure of the fish body length to the blade thickness. In this way, a fast, small fish entering the runner plane is less likely to collide with the blades than a slow, long fish crossing perpendicular to the runner plane. The probabilistic strike frequency (P_{stk}) has been used for fish passage through different systems such as conventional hydropower turbines [24], pumps [25], and hydrokinetic devices [8]. More recently, the effect of leading edge blade thickness (P_{blade}) has been added to compute a combined probability (P) for strike evaluations in conventional hydroelectric turbines [26]. The equation below dictates the probability value:

$$P = P_{stk} + P_{blade} = \frac{n \times N}{V_{axial}} \left(L\cos\left(\alpha\right) + T \right).$$ (1)

Because Eq. 1 requires only a few input parameters, it has been a convenient choice for preliminary evaluations of P based on geometric and rotation rate considerations. We applied the

combined probabilistic model in the example case ($P_{stk} + P_{blade}$) because the blade thickness is radially uniform, and the probabilistic results allowed us to compare the proposed DEM method to simplified passage conditions. More details of the kinematic blade strike model can be found in previous works [16, 17].

Discrete Element Modeling (DEM)

The DEM can evaluate strike frequency by assuming that discrete objects of fish-like shape follow the trajectory of a fish sample that does not include volitional behavior. The DEM consists of computing the finite displacements and rotations of discrete particles [27], and has been popular in fields such as geomechanics and powder technology [15]. The DEM is convenient for the blade-strike frequency evaluation because particle trajectories result from the effects of the flow conditions on the object, as well as from the contact forces on turbine blades. The ability to identify the contact events helps us to determine the number of colliding particles with respect to a released sample.

Once a DEM particle is injected, both the linear and angular momentum balance equations are solved at small time increments to obtain the entire trajectory [28]. The linear momentum equation has the form as in Eq. 2 (see Nomenclature in Appendix A).

$$m_p \frac{d\bar{u}_p}{dt} = \bar{F}_d + \bar{F}_p + \bar{F}_{vm} + \bar{F}_g$$ (2)

The selected forces in eqs. (3) and (11) to (13) are the most influential on particle motion, and follow up with previous solutions with Lagrangian particles [16, 17]. Contact forces were ignored because DEM particle-structure interactions were irrelevant once a contact event was identified and recorded. The drag coefficient (Eqs. 4 through 9) followed the Haider and Levenspiel formulation that was proposed for non-spherical objects in lightly loaded particulate flows, without taking into account the presence of other surrounding particles [29].

$$\bar{F}_d = \frac{1}{2} C_d \rho A_p |\bar{u}_s| \bar{u}_s$$ (3)

$$C_d = \frac{24}{Re_p} \left(1 + ARe_p^B \right) + \frac{C}{\left(1 + \frac{D}{Re_p} \right)}$$ (4)

$$Re_p = \frac{\rho |\bar{u}_s| D_p}{\mu}$$ (5)

$$A = 8.1716e^{-4.0665\phi}$$ (6)

$$B = 0.0964 + 0.5565\phi$$ (7)

$$C = 73.690e^{-5.0746\phi}$$ (8)

$$D = 5.3780e^{6.2122\phi} \tag{9}$$

The linear momentum equation followed the same formulation as in previous applications with Lagrangian particles [16], except for the drag force which was modified by including the effects of the object's sphericity (ϕ). The particle sphericity is the ratio of the surface area of a sphere that has the same volume as the non-spherical object, and is calculated by Eq. 10, where the surface area (A_p) and total volume (V_p) of the composite particle were particle properties available in the software:

$$\phi = \frac{\pi^{1/3}(6V_p)^{2/3}}{A_p} \tag{10}$$

$$\bar{F}_p = -V_p \nabla p_{static} \tag{11}$$

$$\bar{F}_{vm} = C_{vm}\rho V_p \left(\frac{D\bar{u}}{Dt} - \frac{d\bar{u}_p}{dt} \right) \tag{12}$$

$$\bar{F}_g = m_p \bar{g} \tag{13}$$

The equations of motion of DEM particles also included the conservation of angular momentum (Eq. 14) which was only affected by the drag torque produced by the slip-rotation (Eq. 15) following the Sommerfeld formulation in Eq. 16 [30]. Although the original formulation bounds the Re_R (Eq. 17) to values up to 1000, no upper limit was considered in the present implementation.

$$\frac{d}{dt}(\bar{\bar{I}}\bar{\omega}_p) = \frac{\rho}{2}\left(\frac{D_p}{2}\right)^5 C_R |\bar{\Omega}|\bar{\Omega} \tag{14}$$

$$\bar{\Omega} = \frac{1}{2}\nabla \times \bar{u} - \bar{\omega}_p \tag{15}$$

$$C_R = \begin{cases} \frac{12.9}{Re_R^{0.5}} + \frac{128.4}{Re_R}, & 32 \leq Re_R \\ \\ \frac{64\pi}{Re_R}, & Re_R < 32 \end{cases} \tag{16}$$

$$Re_R = \frac{\rho D_p^2 |\bar{\Omega}|}{\mu} \tag{17}$$

FISH SURVIVAL RATE ESTIMATE AND ROTOR AVOIDANCE

The biological performance of a turbine device is complete only when the consequences of the strike events on fish survival are estimated. In the present study, we applied the method described in the previous associated work to estimate fish survival rates from blade-strike [16]. That report outlined the steps involved in the quantitative evaluation of survival rates using the outcomes from Lagrangian particle tracking. In this study, the impact velocities and strike locations are calculated from the DEM particle solutions instead of Lagrangian particles.

The survival rate estimation involves the empirical relationship of the survival rate from a fish sample (SR) as a function of the impact velocity, fish length, and the blade thickness, i.e., $SR = f(\Delta V, L/T)$ [21]. The empirical relationship can be used for the present evaluation because the test conditions in this study were to a large extent similar to laboratory tests for fish length (L = 100-760 mm), impact velocity (ΔV = 3.0-12.2 m/s), and blade thickness (T = 10-150 mm). The survival estimation has been previously implemented for fish survival estimates through conventional hydropower turbines [26].

The survival-estimation method was thoroughly explained in a preceding report openly accessible online [16]. This documents shows the exposure-response relationships, as well as the impact velocity schematic and calculations based on modeled impact data. Here, we will summarize the steps involved in the estimation procedure. The DEM solver recorded the impact velocity (ΔV) and radial distance (R_{stk}) for each colliding particle. The radial location determined the exposure blade thickness of the colliding particle through a function $T = f(R_{stk})$. Thus, the survival probability for each colliding particle was calculated, i.e., $SR = f(\Delta V, L/T)$. Those particles with no collision had a SR = 1.0. The final survival rate was the sum of all individual SR values, divided by the number of particles.

An avoidance rate of 90% was applied to estimate the sensitivity of both blade-strike frequency and survival to a behavioral response of fish near hydrokinetic devices. To do so, the frequency and survival rate were computed based on a randomized sub-sample containing 10% of the full DEM particle sample for each scenario, assuming the remaining to be released but able to entirely evade the runner. This avoidance rate is to a large extent arbitrary, falling between small avoidance values previously accounted for in modeling analyses [5] and those large values found in field studies [22]. The evaluations of survival rates and the inclusion of avoidance rate were carried out for the application case only.

AN EXAMPLE CASE: SIMPLE ROTOR MODEL

The example case allows us to outline the evaluation of blade-strike frequency with the DEM. The primary objective was to ensure that the DEM-based estimates reproduce probabilistic results from Eq. 1. The procedure in both the example and the application cases consists of defining three components: firstly, the composite particle to represent the fish; secondly, the test flow conditions; and thirdly, the injection strategy.

Fish modeled as a DEM composite particle

The practical DEM applications have dealt with non-spherical or irregular bodies by representing them as a compo-
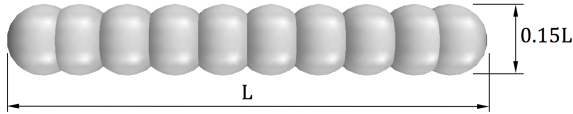
FIGURE 1. The fish was modeled as a particle composed of 10 spheres

FIGURE 2. Simple rotor model with all DEM particles oriented with $\alpha = 45^o$

sition of spheres. Therefore, the fusiform body shape of the majority of fish species can be composed of a large number of particles. As an alternative, formulations have been proposed to compose ellipsoidal particles that follow basic geometric requirements, e.g. aspect ratio [31]. Furthermore, the convenient shape of ellipsoids has motivated studies of ellipsoidal particle motion in laminar [32] as well as turbulent flows [33]. However, a complex body would require a large number of elemental particles which in turn increases the computational expense to calculate the trajectories. The latter computational limits constrain our ability to conduct a statistical study of a large sample. Therefore, the fish body was represented as a composition of 10 spherical particles as shown in Figure 1. The same model was used in both the example and MHK turbine models, although scaled to obtain the test fish lengths.

The example rotor model

The example model consists of one rotating runner with 4 linear blades, placed between two stationary cylindrical regions (Figure 2). The cylinder diameter was 40 cm. All test particles were released with an initial velocity (V_{axial}) of 0.1 m/s. For the example case only, the fluid-particle interaction was not accounted for, thus the flow modeling was not necessary. We tested four parameters to compare DEM-based strike fractions against strike probabilities from Eq. 1: (a) blade thickness, T = 0 cm and 2 cm; (b) rotational speed, n = 0.1 and 0.4 rps; (c) fish length, L = 1 cm and 2 cm; and (d) approaching angle, $\alpha = 0$ and $45°$.

Particles were released from a uniform array of 332 injectors (N_{inj}), covering the entire cross section of the cylinder. However, only a subset of those points was actually selected with an injection probability ($P_{inj} = 0.0025$) every time step ($\Delta t = 0.02$ s) over a period (T_{inj}) of 30 s. With this injection scheme, the total DEM particle sample size for each run was approximately $\frac{N_{inj} \times P_{inj} \times T_{inj}}{\Delta t} = 1245$. The strike fraction ($F_{stk}$) was computed as the ratio of colliding particles to the sample size. A colliding particle was counted once even when it collided on the blades more than once; thus, neither in the example model nor in the application case was the contact physics relevant for this study.
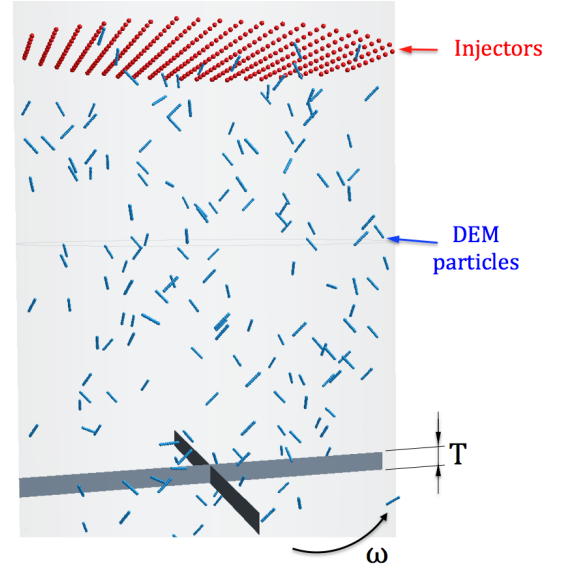
Comparisons: Kinematic Probabilistic vs. DEM modeling

Figure 3 shows that the DEM-based strike ratio is essentially the same as the probabilistic prediction in Eq. 1. Whereas the majority of run cases corresponded to DEM particles crossing perpendicular to the runner plane (filled circles in Fig. 3), a few cases of particles oriented 45° were also simulated (one case shown in Fig. 2, and results indicated as hollow circles in Fig. 3.) The latter cases showed the largest deviation from the bisecting line. This overestimation of the DEM stems from the particle thickness of 15% of the composite particle length (Fig. 1) that is reflected in the DEM scheme but not in the probabilistic model. A confirmation case was run with a "thin" DEM particle with thickness only 3% the fish length (not shown). The results showed that the reduction of particle thickness brings the DEM-based ratio closer to the bisecting line (hollow square in Fig. 3). However, this latter case was computationally demanding because a large number of spheres is necessary to compose one single "thin" particle. Furthermore, the original fish model in Fig. 2 is more valid for the strike frequency evaluation in the application case of MHK turbine flows.

These outcomes demonstrated that the DEM approach, when applied using the simplifying assumptions of the probabilistic model, can correctly capture the geometric aspects of leading edge strike conditions during passage. Even more important is the fact that the DEM approach can also incorporate other conditions —among them the fluid-particle interaction and turbulence— known to have an impact on fish trajectory, strike occurrence, and ultimately on strike-related injury. These ex-

panded capabilities to represent real-word conditions and systems were used in the application case.
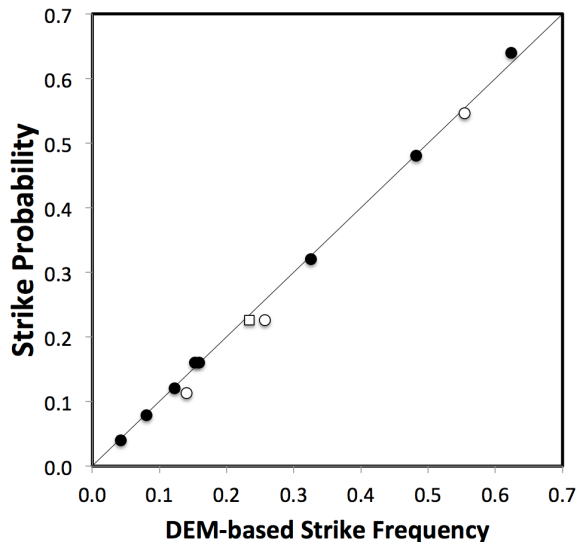
FIGURE 3. Comparisons between Strike Probability from Eq. 1 and DEM-based frequency estimate, for DEM particles both perpendicular (filled circle) and at $\alpha = 45^o$ (hollow circle and square) to the rotor plane

MARINE HYDROKINETIC TURBINE
The MHK turbine characteristics and hydraulic performance: CFD vs. Laboratory experiments

The application case consists of a MHK turbine unit that has been the subject of multi-institutional efforts for design, testing, and evaluation of its hydraulic and environmental performance. The participant institutions include Sandia National Laboratories (design, [34, 35]), UC Davis (blade element method design or BEM, [35]), the Pennsylvania State University (laboratory testing, [36]) and the Pacific Northwest National Laboratory (hydraulic and biological performance assessment, [16, 17, 37]).

The MHK turbine model has three blades with tip radius (R) of 2.44 m and an axis of rotation located 5.16 m above the floor. Other relevant dimensions and features are shown in Fig. 4a and b. Laboratory tests in a water tunnel with a 1:8.7 reduced-scale model (Fig. 4c) evaluated power and thrust coefficients [36, 38]. They are shown in Fig. 4d with respect to the tip speed ratio.

A computational fluid dynamics (CFD) model was set up to simulate the three-dimensional flow and turbulent conditions created by the MHK turbine operation. A commercial CFD package [39] was used to generate a 10.2M-hexahedral-cell mesh of the full-scale MHK unit. The domain was $32 \times 8 \times 16$ runner

diameters (D) in the stream-wise, vertical, and span-wise directions, correspondingly, and was divided into two regions: *(i)* one containing the turbine blades and the volume near the runner, set to rotate with a rigid body motion scheme, and *(ii)* another large stationary region to simulate the flow surrounding the turbine. We ran transient simulations for approaching velocities of 1, 2, and 3 m/s, with a velocity distribution following a power-law relationship in the vertical direction (power coefficient, 0.25) with the nominal velocity at the center of rotation. The runner angular velocity was set at 3.2 rad/s (30.56 rpm) for the three flow simulations. The large turbulent eddies were resolved with the Detached Eddy Simulation (DES, [40]) version of the SST k-ω turbulence model. Inflow turbulence was implemented with the synthetic eddy generation [41] for turbulent conditions previously measured and reported for a tidal site in Puget Sound, Washington (turbulence intensity of 11% and Lagrangian integral time scale of 1.4 s [42]).

An instantaneous visualization of the simulated flow depicts the conditions arising with the combination of unsteady conditions, DES, and synthetic inflow eddy generation (Fig. 5). Comparisons in previous works showed considerable improvement in flow description achieved by the DES scheme over RANS simulations [16]. Transient values of power and thrust reflected the periodicity of flow conditions. As an average, the CFD-simulated power and thrust coefficients were mostly in agreement with the BEM and laboratory results (circles in Fig 4d). We deemed the CFD-simulated conditions acceptable to conduct the strike-frequency evaluation with DEM particles.

We conducted a grid dependency test with a finer mesh of 37.1 M cells, with flow simulation results essentially the same as for the coarser mesh. Further description of the mesh generation, the CFD setup testing, the comparison of CFD vs. laboratory results, the hydraulic performance, the DES method, the inflow turbulence generation, and the comparisons between turbulent approaches can be found in previous works on the same MHK unit at the same flow conditions as in the present application [16, 17]).

DEM Particle Simulation

Flow simulations were run until selected velocity-sampling locations and power calculations showed a statistical steady state of the flow field. This normally took from 60-90 s of simulated real-time. Upon stabilization, the DEM particles were released over a period of 15 seconds from an $20{\times}20$ array of injectors located 10 m upstream from the MHK device. The injectors were arranged at uniform intervals of 30 cm in the vertical and span-wise direction, centered at the axis of rotation. The particle injection rate was 80 per second, the release injector being randomized at each time step ($\Delta t = 0.01$ s). These settings resulted in a total DEM particle sample size of approximately 1200.

The fish length (L in Eq. 1) was a test condition for the

6
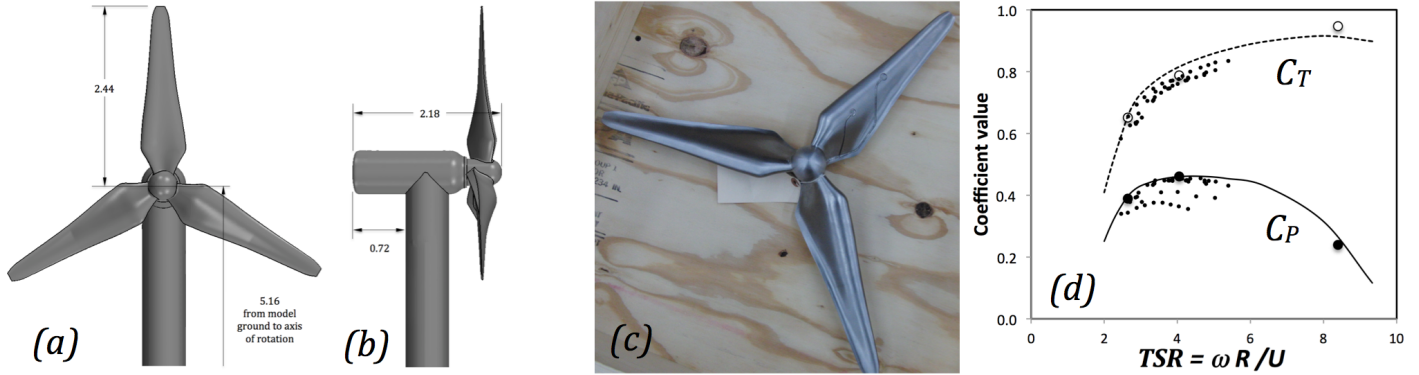
FIGURE 4. The MHK turbine model, (a) front view, (b) side view, (c) laboratory scaled (1:8.7) physical model (PennState), and (d) hydraulic performance of the power (C_P) and thrust (C_T) coefficients from the laboratory data (dots), the BEM results (lines, [35]), and the CFD simulations (hollow and filled circles, [16, 17])

DEM-based strike frequency evaluation. Small (L = 10 cm) and medium size (L = 40.6) fish were of interest in the current application, the former being typical for juvenile migratory salmonids, and the latter being representative of tidal site resident fish. More discussion on the selected fish sizes was provided in the previous studies [16, 17]. The combination of three inflow velocities and two fish lengths gave rise to six simulated scenarios for blade-strike evaluations.

Blade-strike results

The DEM results are summarized in Table 1, and compared against previously reported results [16, 17] in Table 1. Because the MHK runner is not enclosed, only a fraction of the released DEM particle sample had a potential for collision. This potential fraction (in Table 1) was greater at a low approaching velocity (1 m/s) than at high velocities (2 and 3 m/s). However, the potential fraction levels off between the cases for 2 and 3 m/s. Extrapolating this trend for a fish sample, the potential fraction represents those fish that evade the MHK surrounding flow entirely owing to hydraulic conditions; volitional avoidance is not taken into account in this model-based assessment. Laboratory experiments of fish passage through MHK turbines have shown significantly large avoidance rates from fish samples without upstream mesh containment [8]. Therefore, any final judgment of the strike frequency should factor in this type of avoidance for a realistic biological assessment of the MHK turbine.

The strike fraction behaves in a similar manner as the potential fraction: there is a tendency to increased strike rates at 1 m/s, but such tendency becomes less pronounced between the 2 and 3 m/s approaching velocity cases. The magnitude of this trend takes place by holding the same rotor angular velocity across the three inflow velocities; however, if the angular velocity were to increase with the inflow velocity, the strike rates will increase

considerably. Comparing the sensitivity of strike fraction to fish length within each approaching velocity, the low velocity run (1 m/s) produced a proportion between strike fractions ($\sim$3.6x) that nearly reflects the proportion between L values ($\sim$4x). Nevertheless, this proportion was approximately 2.5 in the 2 and 3 m/s cases. This trend reveals that strike frequency is not purely a linear function of the fish length as the simplified formula dictates, but rather depends also on the complex fluid-particle interactions that are accounted for in the DEM-based assessment.

The DEM-based strike frequencies are shown in Table 2. The DEM particles are likely to arrive at the crossing plane not only with an orientation but also with an axial velocity (V_{axial}) component lower than the nominal approaching velocity (U) which in turn increases the likelihood of collision compared to the probabilistic results in previous work [16, 17]. In relation to the Lagrangian particle-based assessment, the DEM scheme represented the entire fish length rather than an equivalent diameter for the spherical Lagrangian particles, thereby increasing significantly the strike frequency. In addition, the Lagrangian solver method tracked only the particle centroid without accounting for the object dimensions. We additionally ran a simulation case to reduce and make the DEM setup equivalent to the Lagrangian particle simulation case of the small fish at 2 m/s. The comparisons showed that the DEM (9.1%) and Lagrangian particles (8.3%) agreed with one another in this comparable instance.

Survival rates based on composite particles are included in Table 2. With the full particle sample (0% avoidance rate), the estimates for small fish (L = 10 cm) indicate a relatively high survival probability in agreement with survival studies with living fish through an axial-flow propeller turbine in laboratory settings [8]. However, the DEM-based survival rates for the mid-size fish were considerably lower than the experimental estimates mostly because of the differences in rotor design. The labora-

7
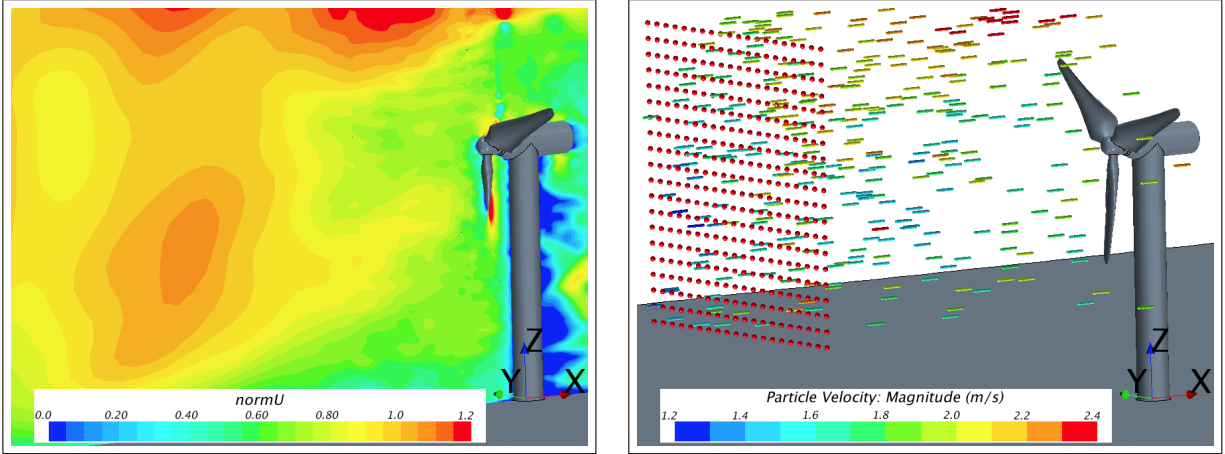
FIGURE 5. Instantaneous flow (top) and DEM particle (bottom, L = 40 cm) solutions four seconds after random injection began from a grid arrangement (red circles) located at 10 m upstream from the turbine. Flow velocities are normalized with respect to the mean inflow velocity, U = 2 m/s

U, m/s	L, cm	Injected particles	With collision potential	Colliding particles	Potential fraction	F_{stk}, %
1	10.0	1227	591	140	48.2	23.7
	40.6	1226	596	403	48.6	67.6
2	10.0	1222	546	73	44.7	13.4
	40.6	1222	553	191	45.3	34.5
3	10.0	1222	546	62	44.7	11.4
	40.6	1221	567	158	46.4	27.9
2	Spheres D = 3 cm	1204	506	46	42.0	9.1

TABLE 1. Summary of DEM simulation results in the MHK model

tory turbine had a tip speed of 2.78 m/s which tended to produce smaller values of blade velocity (V_b), and ultimately, lower impact velocities (ΔV) in comparison to the blade tip speed of 7.88 m/s in the MHK model. The DEM analysis counted only the particles with collision potential, and the laboratory experiments were conducted with upstream containment netting to force fish to pass through the runner. Therefore, neither the DEM-based nor the laboratory estimates accounted for the avoidance rate from volitional behavior of fish in the proximity of operating turbines.

Because laboratory and field evidence showed that virtually all fish were able to avoid the turbine region of influence even when released very close upstream from the runner plane [8, 22], we applied the 90% avoidance rate to the particle sample for each scenario. The results showed both a considerable reduction in strike fraction (nearly responding proportionally to the avoidance rate) and a large increase in survival rate. Therefore, the strong influence of avoidance on the outcomes of this — as well as any other — analysis of strike frequency reinforces the need for fur-

ther quantitative research for other turbine types and arrays of turbines on interactions with fish and other aquatic species [43]. Once avoidance rates are documented for specific species, sites, designs, and flow conditions, they can be included in the presented method for a more representative biological assessment.

The main contribution of the present evaluation of biological performance is to combine modeling capabilities to create a higher degree of real-world representation of MHK turbines. We considered that the DEM-based biological performance assessment of MHK turbines is feasible from the standpoint of available computing infrastructure and CFD modeling capabilities. For instance, each run (one fish size at one approaching velocity) in this study took approximately 60 hr on 36 processors to complete 1 minute of flow and DEM particle simulations. In addition, a number of improvements can be implemented in the DEM scheme, e.g. other composite particle shapes, specific drag force and torque formulations, rebounding particles, among others. The present study —as is— lays out the basis for a higher fidelity of fish passage representation with the corresponding in-

| | | 0% Avoidance | | 90% Avoidance | |
m/s	cm	F_{stk}, %	SR, %	F_{stk}, %	SR, %
1	10.0	23.7	98.5	2.9	99.8
	40.6	67.6	90.3	5.9	99.1
2	10.0	13.4	98.4	1.1	99.1
	40.6	34.5	93.0	4.3	98.7
3	10.0	11.4	99.1	1.6	99.8
	40.6	27.9	94.5	2.8	99.2

TABLE 2. DEM-based strike fractions (F_{stk}) and survival rate (SR), and sensitivity to the avoidance rate

crease in complexity to achieve a solution.

CONCLUSIONS AND FUTURE RESEARCH

This study presented a method to quantitatively evaluate the frequency and severity of fish strikes on marine hydrokinetic devices. The method combined a suite of modeling capabilities such as eddy-resolving flow simulations, actual runner motion, environmental inflow turbulence generation, and discrete-element modeling to determine composite particle trajectories and their interaction with blades. The procedure was outlined with the aid of an example model that showed a strong correlation of the DEM-based strike frequency to a simple probabilistic model widely used for strike evaluations.

One major assumption of this study was that the particle trajectories mimic the potential pathways of fish entrained into the MHK turbine flow. Another assumption was that the particle-structure interactions represented the potential collision events that fish can experience during passage through the runner. Upon these assumptions, the count of collisions from a particle sample allowed for a statistical analysis of the strike frequency for each simulated scenario. Each scenario consisted of the combination of the two test conditions: the fish length (two sizes) and the approaching velocities (three values). The setup and test conditions were based on the design parameters of the actual MHK turbine unit at the expected site and operations. The DEM-based method allowed for estimating the severity of strikes by providing input data to a formulation for survival rate estimates. In addition, the method can accommodate an avoidance rate to test the sensitivity of the estimates to quantifiable parameters indicating fish behavior.

The DEM results demonstrated that the strike frequency was strongly but not linearly related to the fish length, holding the approaching velocity constant. Likewise, the DEM-based strike fractions tended to follow a non-linear correlation to the approaching velocity, holding the fish length constant. In comparison to previous model-based assessments, the DEM scheme produced greater blade-strike frequencies because of its inclusion of both the geometric (as in the probabilistic model) and fluid-particle (as in the Lagrangian-based evaluation) conditions influencing fish passage. Strike-related survival was relatively unaffected by inflow velocity for small fish as compared to mid-size fish. The application of an assumed avoidance rate of 90% resulted in a significant increase of survival rate of nearly 99% across all scenarios. These results point to the need for further research and development of field monitoring methods for operating turbines to better understand the potential interaction between fish and MHK devices [43]. The DEM-based biological performance allows for testing a variety of flows and particle features to reveal those conditions that become hazardous for fish passage.

REFERENCES

[1] Bahaj, A., and Myers, L., 2003. "Fundamentals applicable to the utilisation of marine current turbines for energy production". *Renewable Energy,* **28**(14), Nov, pp. 2205–2211.

[2] Batten, W., Bahaj, A., Molland, A., and Chaplin, J., 2006. "Hydrodynamics of marine current turbines". *Renewable Energy,* **31**(2), Feb, pp. 249–256. 8th World Renewable Energy Congress and Expo, Denver, CO, AUG 29-SEP 03, 2004.

[3] Lago, L. I., Ponta, F. L., and Chen, L., 2010. "Advances and trends in hydrokinetic turbine systems". *Energy for Sustainable Development,* **14**(4), Dec, pp. 287–296.

[4] Mukherji, S. S., Kolekar, N., Banerjee, A., and Mishra, R., 2011. "Numerical investigation and evaluation of optimum hydrodynamic performance of a horizontal axis hydrokinetic turbine". *Journal of Renewable and Sustainable Energy,* **3**(6), Nov.

[5] Schweizer, P. E., Cada, G. F., and Bevelhimer, M. S., 2011. Estimation of the risks of collision or strike to freshwa-

ter aquatic organisms resulting from operation of instream hydrokinetic turbines. FY 2010 Annual Progress Report. Tech. Rep. ORNL/TM-2011/133, Oak Ridge National Laboratory.

[6] Federal Energy Regulatory Commission - Issued Hydrokinetic Projects Preliminary Permits Map. `http://www.ferc.gov/industries/hydropower/gen-info/licensing/hydrokinetics/issued-hydrokinetic-permits-map.pdf`. Accessed: 2014-01-24.

[7] Amaral, S., Hecker, G., and Pioppi, N., 2011. Fish passage through turbines: application of conventional hydropower data to hydrokinetic technologies. Tech. Rep. 1024638, EPRI (Electric Power Research Institute).

[8] Amaral, S., Perkins, N., Giza, D., and McMahon, B., 2011. Evaluation of fish injury and mortality associated with hydrokinetic turbines. Tech. Rep. 1024569, EPRI (Electric Power Research Institute).

[9] Gorlov, A., 2010. Helical turbine and fish safety. Tech. Rep. Half-moon Cove Tidal Power Project P-12704, Tidewalker Associates.

[10] Normandeau Associates, I., 2009. An estimation of survival and injury of fish passed through the Hydro Green Energy Hydrokinetic System, and a characterization of fish entrainment potential at the Mississippi Lock and Dam No. 2 Hydroelectric Project (P-4306), Hastings, MN. Tech. Rep. Project No. 21288, Normandeau Associates, Inc., December.

[11] James, S. C., Seetho, E., Jones, C., and Roberts, J., 2010. "Simulating Environmental Changes Due to Marine Hydrokinetic Energy Installations". In OCEANS 2010, OCEANS-IEEE, IEEE; Marine Technol; OES, pp. 1–10. Washington State Conference and Trade Center (WSCTC), Seattle, WA, SEP 20-23, 2010.

[12] Churchfield, M. J., Li, Y., and Moriarty, P. J., 2013. "A large-eddy simulation study of wake propagation and power production in an array of tidal-current turbines". *Philosophical Transactions of the Royal Society A-Mathematical Physical and Engineering Sciences, 371*(1985, SI), Feb 28.

[13] Harrison, M. E., Batten, W. M. J., and Bahaj, A. S., 2010. "A Blade Element Actuator Disc Approach Applied to Tidal Stream Turbines". In OCEANS 2010, OCEANS-IEEE, IEEE; Marine Technol; OES, pp. 1–8. Washington State Conference and Trade Center (WSCTC), Seattle, WA, SEP 20-23, 2010.

[14] Kang, S., Borazjani, I., Colby, J. A., and Sotiropoulos, F., 2012. "Numerical simulation of 3D flow past a real-life marine hydrokinetic turbine". *Advances in Water Resources, 39*, Apr, pp. 33–43.

[15] Catherine O'Sullivan, 2013. *Particle Discrete Element Modelling: A Geomechanics perspective*. Applied Geotechnics Volume 4. Spon Press.

[16] Richmond, M., Romero-Gomez, P., and Rakowski, C., 2013. Simulating Collisions for Hydrokinetic Turbines. Tech. Rep. PNNL-22580, Pacific Northwest National Laboratory, Richland, Washington. http://www.pnnl.gov/publications/.

[17] Romero-Gomez, P., and Richmond, M. C., 2014. "Simulating blade strike on fish passing through marine hydrokinetic turbines". *Submitted*.

[18] Cada, G. F., and Bevelhimer, M. S., 2011. Attraction to and Avoidance of Instream Hydrokinetic Turbines by Freshwater Aquatic Organisms . Tech. Rep. ORNL/TM-2011/131, Oak Ridge National Laboratory, May.

[19] Schweizer, P. E., Cada, G. F., and Bevelhimer, M. S., 2012. Laboratory Experiments on the Effects of Blade Strike from Hydrokinetic Energy Technologies on Larval and Juvenile Freshwater Fishes. Tech. Rep. ORNL/TM-2012/108, Oak Ridge National Laboratory, March.

[20] Castro-Santos, T., and Haro, A., 2012. Survival and behavior of juvenile Atlantic salmon and adult American shad on exposure to a hydrokinetic turbine. Tech. Rep. 1026904, Electric Power Research Institute.

[21] Amaral, S., and Hecker, G., 2008. Evaluation of the Effects of Turbine Blade Leading Edge Design on Fish Survival. Tech. Rep. 1014937, Electric Power Research Institute.

[22] Hammar, L., Andersson, S., Eggertsen, L., Haglund, J., Gullström, M., Ehnberg, J., and Molander, S., 2013. "Hydrokinetic turbine effects on fish swimming behaviour". *PLoS ONE, 8*(12), 12, p. e84141.

[23] von Raben, K., 1957. "Regarding the problem of mutilations of fishes by hydraulic turbines". *Die Wasserwirtschaft, 4*, pp. 97–100.

[24] Dauble, D., Deng, Z., Richmond, M., Moursund, R., Carlson, T., Rakowski, C., and Duncan, J., 2007. Biological assessment of the advanced turbine design at wanapum dam, 2005. Tech. Rep. PNNL-16682, Pacific Northwest National Laboratory, Richland, WA.

[25] van Esch, B. P. M., 2012. "Fish Injury and Mortality During Passage Through Pumping Stations". *Journal of Fluids Engineering-Transactions of the ASME, 134*(7), Jul.

[26] Richmond, M. C., Rakowski, C. L., Serkowski, J. A., Strickler, B., Weisbeck, M., and Dotson, C. L., 2013. "Design tools to assess hydro-turbine biological performance: Priest Rapids Dam turbine replacement project". In HydroVision 2013.

[27] Cundall, P. A., and Strack, O. D. L., 1979. "A discrete numerical model for granular assemblies". *Géotechnique, 29*(1), pp. 47–65.

[28] CD-adapco, 2013. *User Guide, STAR-CCM+ Version 8.06*. CD-adapco, http://www.cd-adapco.com.

[29] Haider, A., and Levenspiel, O., 1989. "Drag coefficient and terminal velocity of spherical and nonspherical particles".

Powder Technology, 58(1), pp. 63 – 70.

[30] Sommerfeld, M., 2000. Theoretical and Experimental Modelling of Particulate Flows. Tech. Rep. Lecture Series 2000-06, von Karman Institute for Fluid Dynamics, Sint-Genesius-Rode, Belgium.

[31] Markauskas, D., Kačianauskas, R., Džiugys, A., and Navakas, R., 2010. "Investigation of adequacy of multi-sphere approximation of elliptical particles for dem simulations". *Granular Matter, 12*(1), pp. 107–123.

[32] Jeffery, G. B., 1922. "The motion of ellipsoidal particles immersed in a viscous fluid". *Proceedings of the Royal Society of London. Series A, 102*(715), pp. 161–179.

[33] Zhang, H., Ahmadi, G., Fan, F.-G., and McLaughlin, J. B., 2001. "Ellipsoidal particles transport and deposition in turbulent channel flows". *International Journal of Multiphase Flow, 27*(6), pp. 971 – 1009.

[34] Barone, M., 2010. Preliminary Design of a Reference Marine Hydrokinetic Turbine. Tech. rep., Sandia National Laboratories, Albuquerque, NM.

[35] Shiu, H., van Dam, C., Barone, M., Johnson, E., Phillips, R., Straka, W., Fontaine, A., and Jonson, M., 2012. "A Design of a Hydrofoil Family for Current-Driven Marine Hydrokinetic Turbines". In ICONE20, ICONE20POWER, pp. 1–9. Anaheim, CA, JUL 30 - AUG 3, 2012.

[36] Fontaine, A. A., Straka, W. A., Meyer, R. S., and Jonson, M. L., 2013. A 1:8.7 scale water tunnel verification and validation test of an axial flow water turbine. Tech. Rep. TR 13-002, Applied Research Laboratory at The Pennsylvania State University.

[37] Richmond, M., Rakowski, C., Perkins, W., and Serkowski, J., 2010. Simulating Collisions for Hydrokinetic Turbines. FY2010 Annual Progress Report. Tech. Rep. PNNL-19860, Pacific Northwest National Laboratory, Richland, Washington. http://www.pnnl.gov/publications/.

[38] Neary, V., Fontaine, A., Bachant, P., Gunawan, B., Wosnik, M., Michelen, C., Meyer, R., and Straka, W., 2013. "US Department of Energy (DOE) National Lab Activities in Marine Hydrokinetics: Scaled Model Testing of DOE Reference Turbines". In European Wave and Tidal Energy Conference. Aalborg, Denmark.

[39] CD-adapco, 2013. *User Guide, STAR-CCM+ Version 8.02*. CD-adapco, http://www.cd-adapco.com.

[40] Spalart, P. R., 2009. "Detached-Eddy Simulation". *Annual Review of Fluid Mechanics, 41*, pp. 181–202.

[41] Jarrin, N., Benhamadouche, S., Laurence, D., and Prosser, R., 2006. "A synthetic-eddy-method for generating inflow conditions for large-eddy simulations". *International Journal of Heat and Fluid Flow, 27*(4), Aug, pp. 585–593. 4th International Symposium on Turbulence and Shear Flow Phenomena, Williamsburg, VA, JUN 27-29, 2005.

[42] Thomson, J., Polagye, B., Durgesh, V., and Richmond, M. C., 2012. "Measurements of Turbulence at Two Tidal Energy Sites in Puget Sound, WA". *IEEE Journal of Oceanic Engineering, 37*(3), Jul, pp. 363–374.

[43] Polagye, B., Copping, A., Suryan, R., Kramer, S., Brown-Saracine, J., and Smith, C., 2014. Instrumentation for Monitoring around Marine Renewable Energy Converters: Workshop Final Report. Tech. Rep. PNNL-23100, Pacific Northwest National Laboratory, Richland, Washington. http://www.pnnl.gov/publications/.

Appendix A: Nomenclature

P	Strike probability
P_{stk}	Strike probability owing to the leading edge
P_{blade}	Strike probability owing to the blade thickness
n	Rotational speed of runner, rpm
N	Number of blades
V_{axial}	Fish velocity perpendicular to runner plane, m/s
L	Fish length, m
α	Fish orientation with respect to runner plane, °
T	Blade thickness, m
m_p	Particle mass, kg
$\bar{u}_p$	Particle velocity vector, m/s
$\bar{F}_d$	Drag force, N
$\bar{F}_p$	Pressure gradient force, N
$\bar{F}_{vm}$	Virtual mass force, N
$\bar{F}_g$	Gravity force, N
C_d	Modified drag coefficient for composite particle
ρ	Fluid density, kg/m^3
$\bar{u}_s$	Slip velocity vector, m/s
Re_p	Particle Reynolds number
D_p	Equivalent particle diameter, m
μ	Fluid dynamic viscosity, Pa · s
ϕ	Sphericity
A_p	Composite particle surface area, m^2
V_p	Particle volume, m^3
p$_{static}$	Static pressure, N
C$_{vm}$	Virtual mass coefficient, $C_{vm} = 0.5$
$\bar{u}$	Flow velocity, m/s
$\bar{g}$	Gravity, m/s^2
$\bar{\bar{I}}$	Diagonal tensor of principal moment of inertia, kg/m^2
$\bar{\omega}_p$	Particle angular velocity, rad/s
C_R	Rotational drag coefficient
Re_R	Rotational Reynolds number
$\bar{\Omega}$	Slip-rotational velocity, rad/s
ΔV	Impact velocity, m/s
R_{stk}	Radial location of strike, m
SR	Survival rate, %
U	Approaching velocity, m/s